X-913-74-113
PREPRINT

ESTIMATION OF SUNLIGHT PENETRATION IN THE SEA FOR REMOTE SENSING

W. R. McCLUNEY

APRIL 1974

GODDARD SPACE FLIGHT CENTER
GREENBELT, MARYLAND

ESTIMATION OF SUNLIGHT PENETRATION IN THE SEA FOR REMOTE SENSING

W. R. McCluney

Hydrology and Oceanography Branch

NASA/Goddard Space Flight Center

April 1974

GODDARD SPACE FLIGHT CENTER

Greenbelt, Maryland

ESTIMATION OF SUNLIGHT PENETRATION IN THE SEA FOR REMOTE SENSING

W. R. McCluney

Hydrology and Oceanography Branch, Code 913

NASA/Goddard Space Flight Center

Greenbelt, Md. 20771

ABSTRACT

There is a need for a simple theoretical approach to the calculation of sunlight penetration depths suitable for passive multispectral remote sensing of water resources. An earlier paper presented an approach which is readily adapted to this calculation and which provides reasonably good agreement with more accurate but time-consuming radiative transfer models. The needed modifications are described and the model is used to calculate the penetration of sunlight into clear ocean water at several wavelengths throughout the visible portion of the spectrum. Calculations for both clear and turbid water are carried out for the two visible channels of the multispectral scanner on NASA's ERTS-1 satellite. The effect of a reflective bottom on the upwelling light field is discussed. Measurement parameters needed for the passive remote determination of water depths are identified and the use of submerged reflective panels for surface truth measurements is discussed.

INTRODUCTION

A number of investigators are using the Multispectral Scanner Subsystem (MSS) on NASA's Earth Resources Technology Satellite (ERTS-1) for remote sensing of water resources.[1] In many of these investigations it is necessary to have a rough idea of the effective penetration depth of imagery in each of the spectral bands employed by the MSS. Klemas has devised a slanting board with painted stripes chosen to match the two visible channels of the MSS and calibrated to give a visual estimate of this penetration depth.[2] Other investigators use a white circular disk, called a Secchi disk, lowered into the water until it disappears from view in order to obtain approximate information as to the penetration of sunlight into the water. The Secchi disk has been widely used in oceanography for measurements of water transparency. Some ERTS investigators are attempting to use the upwelling light reflected from a shallow bottom to estimate water depths.

In each of the above investigations, there is a need for simple theoretical techniques relating the observations to the optical properties of both the water and the submerged reflecting surfaces. In a recent paper[3] an optical model developed by Hansen[4] and Gordon[5] was used to calculate the upwelling spectral radiance emerging from the sea. Although the accuracy of the model is limited by the simplifying assumptions upon which it is based, it is superior to single-scattering models for calculations of ocean color spectra and is easily adpated

to the calculations needed here. The purpose of this paper is to illustrate the use of the model in estimating depths of sunlight penetration in typical remote sensing situations.

PENETRATION DEPTH CALCULATIONS

With a few modifications of the equations presented in reference 3 we can obtain analytical expressions for the reflectance of the sea and the apparent brightness of submerged reflecting panels as functions of depth. Skylight contributes less than 30% of the total upwelling radiance emerging from beneath the sea. We may, therefore, further simplify our calculations by neglecting this contribution and consider only the penetration of sunlight into the sea. The upwelling radiance predicted by the single-scattering model for this case is given by equation (8) in reference 3. For a single, homogeneous layer of depth z in the sea, illuminated by the sun at an angle of θ from the nadir (the solar zenith angle is $\pi - \theta$), this equation may be written as

$$R(\lambda) = \frac{N(\lambda)}{H_0(\lambda)} = \frac{T_0 T(\theta)\, \beta(\lambda, \theta')\, [1 - e^{-cz(1-\sec\theta')}]}{\eta^2\, (1 - \cos\theta')\, c(\lambda)} \qquad (1)$$

Equation (1) gives the nadir-viewed upwelling spectral radiance $N(\lambda)$ emerging from the sea divided by the incident solar irradiance $H_0(\lambda)$ at wavelength λ. This ratio will be called the radiance reflectance, $R(\lambda)$, throughout this paper. T_0 is the transmittance of the air-sea interface for upwelling light, T is

the transmittance for downwelling sunlight, H_0 is the spectral irradiance on a horizontal plane due to incident sunlight, η is the index of refraction of seawater, β is the spectral volume scattering function, and c is the single scattering extinction coefficient. The quasi-single scattering extinction coefficient c* is defined to be $c(1 - \omega_0 F)$, where ω_0 is the single scattering albedo and F is the forward scattering coefficient. Replacing c by c* in equation (1) converts it to the quasi-single scattering case described in reference 3. θ' is the angle in water made by the rays of the sun with respect to the zenith. It is related to θ by Snell's law: $\eta \sin(\pi - \theta') = \sin(\pi - \theta)$. We are here assuming a perfectly smooth sea surface.

We shall examine the predictions of eq. 1 for clear ocean water. In evaluating equation 1 we use the usual Fresnel reflectance formula for calculating the transmittances T_0 and T. For $\theta = 150°$, as is approximately the case with ERTS-1 when it crosses the central latitudes of the U.S., we have $T_0 = .9796$ and $T(150°) = .9785$. All of these quantities are defined in reference 3.

The data we shall use for $c(\lambda)$ and $\omega_0(\lambda)$ in our simulation are taken from a paper by Tyler, Smith, and Wilson[6] for clear water optically similar to that found in the Sargasso Sea. Data for β is taken from measurements of the scattering function in the Sargasso Sea made by Kullenberg.[7] The index of refraction of the sea water, η, is approximately 4/3 and is not strongly wavelength dependent in the visible portion of the spectrum. The forward scattering

coefficient F is calculated from by straightforward numerical integration. We shall determine the radiance reflectance using equation 1 at 450 nm, which is close to the wavelength of maximum transparency of the sea, and for a zenith sun.

The results of this calculation, using Eq. (1), are shown in Figure 1 for both the single-scattering (SS) case and for the quasi-single scattering (QSS) case (when c* is used for c in Eq. 1).

We see from this figure that the light penetrates deeper and produces a stronger return signal with the QSS model than with the SS model. The depth for the radiance reflectance to reach 90% of its maximum value is about 25 meters, according to the QSS model. We can also see from this figure the importance of including the effects of multiple scattering in calculations of penetration depths when ω_0 is large.

In order to extend these results to other wavelengths in the spectrum, the Kullenberg scattering data at 460 and 655 nm was linearly interpolated to give values for β at 450, 500, 550, 600, and 650 nm. In addition, the function at 350 and 400 nm was set equal to that at 450 nm and at 700 nm it was set equal to that at 650 nm. The results for the quasi-single scattering model are shown in Figure 2. We see that the upwelling red light reaches a maximum quickly, in less than one meter of depth. The reflectance is correspondingly low for this color. Blue light penetrates much more deeply and returns a stronger signal.

From Figures 1 and 2 we can see the decreasing importance of deeper and deeper layers to the upwelling radiance spectrum. Since in reality the optical properties of the ocean vary with depth, when one measures an ocean color spectrum he obtains a weighted average of these properties over depth. If the depth dependence of these properties is known, then it may be accounted for by replacing equation (1) with

$$R(\lambda) = \frac{T_0 T(\theta)}{\eta^2 \cos \theta'} \int_0^z \gamma(\lambda, \theta', z) \exp\left[-(1 - \sec\theta') \int_0^{z'} c^*(z'')\, dz''\right] dz'. \qquad (2)$$

To show more explicitly the wavelength variation of the penetration, the radiance reflectance calculations were used to determine the layer depth for which the upwelling radiance is 90% of its maximum value. The resulting so-called "penetration depths" are listed in Table 1. This data applies to clear ocean water only. Also given are the SS and QSS attentuation lengths 1/c and 1/c*, respectively, and the approximate horizontal visibility distance using Duntley's criterion. These results are plotted in Figure 3.

ERTS PENETRATION DEPTHS

We shall apply the above results to the two visible-wavelength bands of the ERTS-1 MSS. The "green" band, covering the spectral range 500-600 nm, is called band 4 in the ERTS Data User's Handbook.[9] The red band, covering 600-700 nm, is called band 5. In performing this calculation,

we again used the Tyler, Smith, and Wilson data[6] to calculate $c(\lambda)$ and $\omega_0(\lambda)$ at 20 nm intervals over the range from 500 to 700 nanometers. The scattering functions used in the previous section were linearly interpolated to obtain β at the same wavelengths used for $c(\lambda)$ and $\omega_0(\lambda)$. The resulting radiance reflectances were then averaged over the two ERTS-1 MSS visible wavelength bands separately. The results are plotted in Figure 4 for a 30° zenith sun angle and for nadir viewing.

We see in Figure 4 that the SS model is adequate for band 5 but the QSS model should be used in calculating band 4 penetration depths. The depths for 90% of maximum radiance reflectance are approximately 18 and 3.8 meters for bands 4 and 5, respectively, using the predictions of the QSS model. The low penetration of band 5 is due primarily to a high extinction coefficient for sea water over the wavelength range of this band.

Since most ERTS-1 oceanographic investigations are concerned with coastal waters, which are generally more turbid than open ocean waters, the above results will be of limited usefulness, other than to indicate the clear water limit of sunlight penetration into the sea. In order to provide an estimate of the results one might obtain in a more turbid area, we turn to the measurements of β and c made by Petzold at 515 and 520 nm, respectively, in the relatively turbid waters of San Diego harbor.[10] Although significant variations in the shapes of the wavelegnth spectra of β and c are known to occur when going from clear to turbid water, lack of suitable measurements of these variations compels us to assume that the changes are negligiable. Since we are mostly concerned with

obtaining an estimate of the range of penetration depths which might be found with ERTS-1 imagery, the crudeness of our assumption should not be too onerous.

The total scattering coefficient b is defined by the relation

$$b = \int_0^{4\pi} \beta(\psi)\, d\omega = 2\pi \int_0^{\pi} \beta(\psi) \sin\psi \, d\psi$$

where ψ is the scattering angle. Petzold obtained a value of 1.824 for b at 515 nm. For c he measured 2.19 at 530 nm, giving an approximate ω_0 of 0.833. The values for b, c, and ω_0 at 500 nm used in the above clear water simulation were 0.03234, 0.0846, and 0.3823, respectively. The turbid (San Diego Harbor) – to – clear (Sargasso Sea) – water ratios of these quantities are 56.4, 25.8, and 2.18, respectively. By multiplying the clear water values for β and c by these ratios at each of the wavelengths from 500 nm to 700 nm used in the previous simulation, we obtain a crude representation of the required data for turbid water. Repeating the calculations that led to figure 4, but using our simulated turbid water data, yields the results shown in Figure 5. The corresponding QSS 90% penetration depths for bands 4 and 5 are 1.8 and 0.16 meters, respectively.

As expected, the depth of penetration is very much less for turbid water than for clear ocean water. Although this calculation is only approximate, it should give at least an order-of-magnitude estimate for turbid estuarine water.

By using better data for c and r_0, the accuracy of the estimate can be greatly improved.

REFLECTION FROM A SHALLOW BOTTOM

If the lower surface of the ocean is partially reflecting, as would be the case with a shallow bottom or a submerged reflecting panel, then additional terms must be added to equation 1 to account for the additional flux reflected from the bottom. If this surface is a lambertian reflector, with its diffuse irradiance reflectivity given by $r_0(\lambda)$ (defined to be the ratio of upwelling to downwelling spectral irradiance just above the surface), and if we ignore the multiple reflections between the bottom and the water-air interface, then the added contribution to the upwelling radiance reflectance above the sea can be written in the quasi-single scattering approximation as

$$R_0(\lambda) = \frac{T_0 T(\theta)}{\pi \eta^2} \, r_0(\lambda) \, e^{-c^*(\lambda)(1-\sec\theta')z}, \tag{3}$$

where z is the bottom depth. Adding (3) to equation (1) (with c replaced by c*) gives the radiance reflectance for an ocean having a reflective bottom of irradiance reflectivity r_0 at depth z:

$$R(\lambda) = \frac{T_0 T(\theta)}{\eta^2} \left[\frac{\beta(\lambda\,\theta')\,[1 - e^{-c^*(1-\sec\theta')z}]}{c^*(1-\cos\theta')} + \frac{r_0(\lambda)}{\pi} \, e^{-c^*(1-\sec\theta')z} \right]. \tag{4}$$

The limitations of this expression must be pointed out. Firstly, QSS calculations of the downwelling, forward-scattered (and unscattered) light field are not expected to be as accurate, due to the nature of the QSS assumptions (given in ref. 3), as were the calculations of the upwelling, backward-scattered light field discussed in the previous section. In the presence of a reflecting bottom, this downwelling light field will be re-directed upwards and will combine with path radiance due to backscattering to produce the upwelling radiance spectrum emerging from the water. Thus, any inaccuracy in the predictions of the downwelling light field will be present in predictions of the bottom-reflected portion of the upwelling light field (given by eq. (3)). Thus, we cannot expect as good an agreement between the QSS model and more rigorous radiative transfer calculations when the emerging light reflected from the bottom is a substantial fraction of the total upwelling light field.

These observations have been confirmed by Gordon. He has found that the QSS model predicts a radiance reflectance due to the bottom only which is 20% less than that predicted by his Monte-Carlo radiative transfer calculation, for the case $\omega_0 = 0.2$, a bottom albedo of unity, and a bottom depth of one optical thickness.[11,12]

Another source of error can be identified which is not accounted for in the above calculations. When the bottom is bright and the water is clear and shallow, some of the light reflected from the bottom will be reflected downward by the air-water interface and will be again reflected by the bottom. This contribution, and the error it produces, will be substantial whenever the bottom depth is small.

Due to these limitations, equation (4) cannot be expected to give accurate predictions of the upwelling radiances in the presence of a shallow bottom with high reflectivity. We can, however, use equation (4) to discuss in a qualitative way the various functional dependencies between the upwelling light field and the various subsurface parameters influencing it.

For example, let us examine the predictions of this expression for passive remote determinations of bottom depth. If one wishes to determine z from measurements of $R(\lambda)$, using equation (4), then $r_0(\lambda)$ and the depth dependence of both $\beta(\lambda,\theta')$ and $c(\lambda)$ would have to be measured as well. This requirement greatly restricts the usefulness of the technique. But if several wavelengths are used, and a few simplifying assumptions are made, then it becomes theoretically possible to determine the depth with substantially less information being required. For example, suppose we limit our measurements to areas where the water is homogeneous and is sufficiently clear and shallow that the light from the bottom is much stronger than that scattered upward by the water. In this case the first term in equation (4) may be neglected and we are left with equation (3). Now let us suppose that measurements of $R(\lambda)$ are made at two wavelengths, designated λ_1 and λ_2. Writing equation (3) for each of these and then dividing the one for λ_1 by the one for λ_2, and solving for z, yields the expression:

$$z = \frac{1}{[c^*(\lambda_1) - c^*(\lambda_2)](1 - \sec\theta)} \ln\left[\frac{r_0(\lambda_1)}{R(\lambda_1)} \frac{R(\lambda_2)}{r_0(\lambda_2)}\right]. \qquad (5)$$

Using this expression, we only need to know the difference in quasi-single-scattering extinction coefficients and the ratio of r_0 to R at the two wavelengths in order to determine the depth. The single scattering version of this expression has been used by Polcyn and Lyzenga to estimate bottom depths in the Bahama islands using ERTS imagery.[13]

Although the accuracy of Equation (5) is limited, as was discussed before, it can be used to identify several potential sources for considerable error which would be present in calculations based on similar approaches. For example, an undetected change in the shape of the bottom reflectivity spectrum would be erroneously detected as a change in the water depth. An unexpected increase in water turbidity could be incorrectly interpreted as a decrease in bottom depth.

The difficulty of finding water of sufficient shallowness and clarity that the first term of equation (4) may be neglected makes this approach to accurate passive remote determinations of bottom depth rather unattractive, even if a rigorous radiative transfer calculation were used in place of the present approximate analysis.

By dropping the assumption that the water is shallow and clear enough to neglect the first term of equation (4), and by assuming that measurements will be made of $c(\lambda)$, $\beta(\lambda,\theta')$, and $r_0(\lambda)$ at several wavelengths for some point in the field of view of the remote sensor, then the more generally valid equation (4)

can be used. However, the potential errors produced by unaccounted for changes in bottom reflectivity and water turbidity away from the surface measurement location will persist, and, in the author's view, will severly limit the usefulness of the technique for routine measurements of bottom depth with the kind of regularity and accuracy which is desired. Any attempt to make passive remote measurements of water depths must recognize the need for a number of optical measurements at the surface and the limitations of accuracy which will be imposed by the absence of any of those measurements.

REFLECTION FROM SUBMERGED REFLECTING PANELS

Let use now use equation (4) to determine the depth dependence of the upwelling spectral radiance integrated over bands 4 and 5 of the ERTS-1 MSS for the case of submerged reflecting panels of known spectral reflectance $r_0(\lambda)$. We shall assume that the panel reflectance is constant over the wavelength ranges involved. Using the clear and turbid ocean cases described earlier, and evaluating equation 4 with assumed bottom albedos r_0 of zero, 0.1, 1, 10, 20, 40, and 60 percent, we obtain the results shown in Figures 6 and 7.

We must again point out the limitations of these results. Although they should be more accurate than those obtained using the single-scattering approximation alone, the results do not fully and accurately account for the effects of multiple scattering within the medium and they totally neglect the multiple reflections taking place between the bottom and the surface. Nevertheless, Figs. 6 and 7 can be used to illustrate the general behavior of the radiance reflectances

with increasing depth. At very great depths, the reflecting panels effectively disappear and we are left with the more accurate case of an infinitely deep ocean described in reference (3).

Looking at the results shown in Figures 6 and 7, we see immediately that the use of a reflective panel having a reflectance of 20% or greater can significantly extend the apparent depth of penetration of sunlight into the sea. Visual estimates of this penetration depth using reflecting panels or colored Secchi disks will depend upon the visual contrast of the submerged target, which will in general appear to decrease in size with increasing depth. The results shown in Figs. 6 and 7, however, are based upon the implied assumption that the horizontal dimensions of the submerged panel are substantially greater than the depths at which it is used. It is therefore difficult to relate the results of Figs. 6 and 7 to the disappearance of a panel from view. Thus, great care must be taken when using Secchi disks or reflecting panels in attempts to estimate depths of sunlight penetration application to remote imagery of water resources.

The measurement of Secchi depth is subject to a number of extraneous influences, most notably the disruption of the image due to surface waves, the extent of obscuration of the sun due to atmospheric haze, clouds, or overcast, and variations in the visual acuity of individual observers. As a result, the Secchi depth measurement is extremely subjective and inaccurate, and can be regarded as little more than a qualitative estimate of water clarity.

The inclined submerged reflecting panel, properly used, can be a powerful surface truth technique in remote sensing situations. If its reflectance spectrum $r_0(\lambda)$ is known accurately, and if its horizontal dimensions are much greater than the depths at which it is used, then, with a suitably designed radiometer it should be possible to obtain the full depth dependence of the radiance reflectance $R(\lambda)$ approximated by equation (4). For very small values of z, to a first approximation the second term dominates and it might be possible to use the measurements of $R(\lambda)$ in this range to determine the QSS extinction coefficient c^*.

For increasing values of z, the first term in eq. (4) will have a growing influence. The value of c^* obtained from the measurements at small values of z can be substituted into this equation and an estimate of the volume scattering function β may be thereby obtained at the wavelength and scattering angle involved. The technique requires accurate knowledge of the downwelling sunlight spectral irradiance and it cannot be used if the sky is hazy or overcast. The presence of skylight can significantly influence the results, especially at shorter wavelegths, and should be carefully considered in any intended application of the technique.

CONCLUSIONS

We have shown the utility of the quasi-single scattering model for calculating the penetration of sunlight into natural waters. Although the accuracy of the

model is still not optimal, it is superior to single-scattering models for these calculations. The lack of accurate extinction and scattering data is at present the primary factor limiting the accuracy of the approach when applied to practical situations.

For more accurate calculations of the upwelling radiance spectrum emerging from natural waters, or of the penetration depth spectrum, one must have the full wavelength dependence of both the extinction coefficient and the volume scattering function (over its full angular range) for the body of water being modeled, regardless of the particular theoretical model being used. This information can come from measurements made in the field or it can be of a suitably formulated microscopic model of the optical properties of the water, as described in ref. 3. It is essential that progress be made either in developing the microscopic model or in providing the instrumentation needed to gather the information directly if accurate upwelling radiance spectra and penetration depths are to be calculated. This conclusion applies as strongly when a shallow bottom is present. And in this case it is also necessary to have the spectral reflectance of the bottom.

When the water color spectrum is being modeled in shallow water, the QSS approximation leads to some improvement over simple, single-scattering theories, but it fails to fully account for the effects of multiple scattering. And, as used in this paper, it totally neglects multiple reflections between the bottom

and the water surface. Nevertheless, the QSS model provides a framework for identifying potential sources of error in passive remote measurements of bottom depth.

If a sufficiently homogeneous body of water could be found, it might be possible to measure the surface parameters needed for the calculations at one (or several) location in the viewed area and to use the remote data to extrapolate to other locations. But waters of sufficient homogeneity are relatively rare in the world oceans. Even when homogeneous waters can be found, there still exists the potential for undetected changes in water turbidity, and hence some uncertainty in the depth calculations.

A conceivable, though not very likely, solution to the problem might be the existence of fundamental (though empirical) relationships of biological-chemical-optical origin, which can be used to connect the degree of water turbidity (or bottom albedo) with observed spectral changes. If such relationships could be discovered, they could be used to detect changes in bottom albedo or water turbidity remotely without the need for surface detection of these changes.

Although the existence of these relationships appears to be somewhat unlikely, owing to the complexity of the biological, chemical, and optical processes involved, nevertheless, an experimental program aimed at thier discovery would be a worthwhile task.

ACKNOWLEDGEMENTS

The author would like to acknowledge many helpful discussions with H. R. Gordon of the University of Miami, and to thank him and O. B. Brown for making available some preliminary results of their Monte-Carlo radiative transfer model.

References

1. Proceedings of the Symposium on Significant Results Obtained from the Earth Resources Technology Satellite-1, 5-9 March 1973, NASA/Goddard Space Flight Center, Greenbelt, Md. 20771, Vol. I., publication no. NASA SP-327, available from U. S. Gov. Print. Off., Washington, D. C. 20402, GPO cat. no. NAS 1.21:327.

2. V. Klemas, J. F. Borchardt, and W. M. Treasure "Suspended Sediment Observations from ERTS-1," Rem. Sens. of Environ. 2, 205 (1973).

3. W. R. McCluney, "Ocean Color Spectrum Calculations," February 1974, Doc. No. X-913-74-53, Goddard Space Flight Center, Greenbelt, Maryland 20771.

4. J. E. Hansen, "Multiple Scattering of Light in Planetary Atmospheres. Part II. Sunlight Reflected by Terrestrial Water Clouds" J. Atmos. Sci. 28, 1400 (1971), See eqs. (9-11), p. 1420.

5. H. R. Gordon, "A Simple Calculation of the Diffuse Reflectance of the Ocean" to be published in Appl. Opt. 13, (1974).

6. J. E. Tyler, R. C. Smith, and W. H. Wilson, "Predicted Optical Properties for Clear Natural Water," J. Opt. Soc. Am. 62, 83 (1972).

7. Gunnar Kullenberg, "Scattering of Light in Sargasso Sea Water," Deep Sea Research 15, 423 (1968).

8. S. Q. Duntley, "Light in the Sea" J. Opt. Soc. Am. 53, 214 (1963).

9. NASA Earth Resources Technology Satellite Data Users Handbook, Doc. No. 715D4249, Goddard Space Flight Center, Greenbelt, Md. 20771, avail. from ERTS Liason Office, General Electric Co., 5030 Herzel Pl., Beltsville, Md. 20705.

10. T. J. Petzold, "Volume Scattering Functions for Selected Ocean Waters," Visibility Laboratory Technical Report No. 72-78, Scripps Institution of Oceanography, San Diego, Calif. 92152, 75 pp.

11. H. R. Gordon and O. B. Brown, "Irradiance Reflectivity of a Flat Ocean as a Function of Its Optical Properties," Appl. Opt. 12, 1549 (1973).

12. H. R. Gordon, Dept. of Physics, Univ. of Miami, Coral Gobles, Fla. 33124, private communication.

13. F. C. Polcyn and D. R. Lyzenga, "Calculations of Water Depth from ERTS-MSS Data, "Proceedings of the Symposium on Significant Results Obtained from the Earth Resources Technology Satellite-1, NASA/Goddard Space Flight Center, Greenbelt, Md. 20771, publication no. NASA SP-327.

TABLE I

MACROSCOPIC MODEL PENETRATION DEPTHS

CLEAR OCEAN WATER

Wavelength	350	400	450	500	550	600	700	NM
1 : C	8.6	10.8	12.2	11.8	9.2	3.9	1.5	Meters
S.S. Penetration Depth[a]	9	12	15	14	11	4	1.8	Meters
1 : C*	21.4	25.7	26	21.2	13.4	4.4	1.6	Meters
Q.S.S. Penetration Depth[a]	13	18	22	21	14	6	1.8	Meters
Approximate horizontal visibility distance (4 : C)	34	43	49	47	37	16	6	Meters

[a]Layer depth for which upwelling radiance reflectance is 90% of its maximum value.

Figure Captions

Figure 1. A comparison of SS and QSS Models in predictions of the radiance reflectance as a function of layer depth for clear ocean water at 450 nm with a zenith sun.

Figure 2. QSS Model predictions of the radiance reflectance as a function of layer depth for clear ocean water at several wavelengths and for a zenith sun.

Figure 3. SS and QSS model penetration depths for clear ocean water as a function of wavelength for a zenith sun, no atmosphere, and a smooth sea surface.

Figure 4. SS and QSS Model radiance reflectance versus layer depth averaged over the two visible-wavelength ERTS-1 MSS bands for clear ocean water and a solar zenith angle of 30 degrees.

Figure 5. SS and QSS Model radiance reflectances versus layer depth averaged over the two-visible-wavelength ERTS-1 MSS bands for turbid water and a solar zenith angle of 30 degrees.

Figure 6. QSS Model radiance reflectances versus layer depth averaged over the ERTS-1 MSS bands for clear water and several different bottom albedos, r_0.

Figure 7. QSS model radiance reflectances versus layer depth averaged over the ERTS-1 MSS bands for turbid water and several different bottom albedos, r_0.

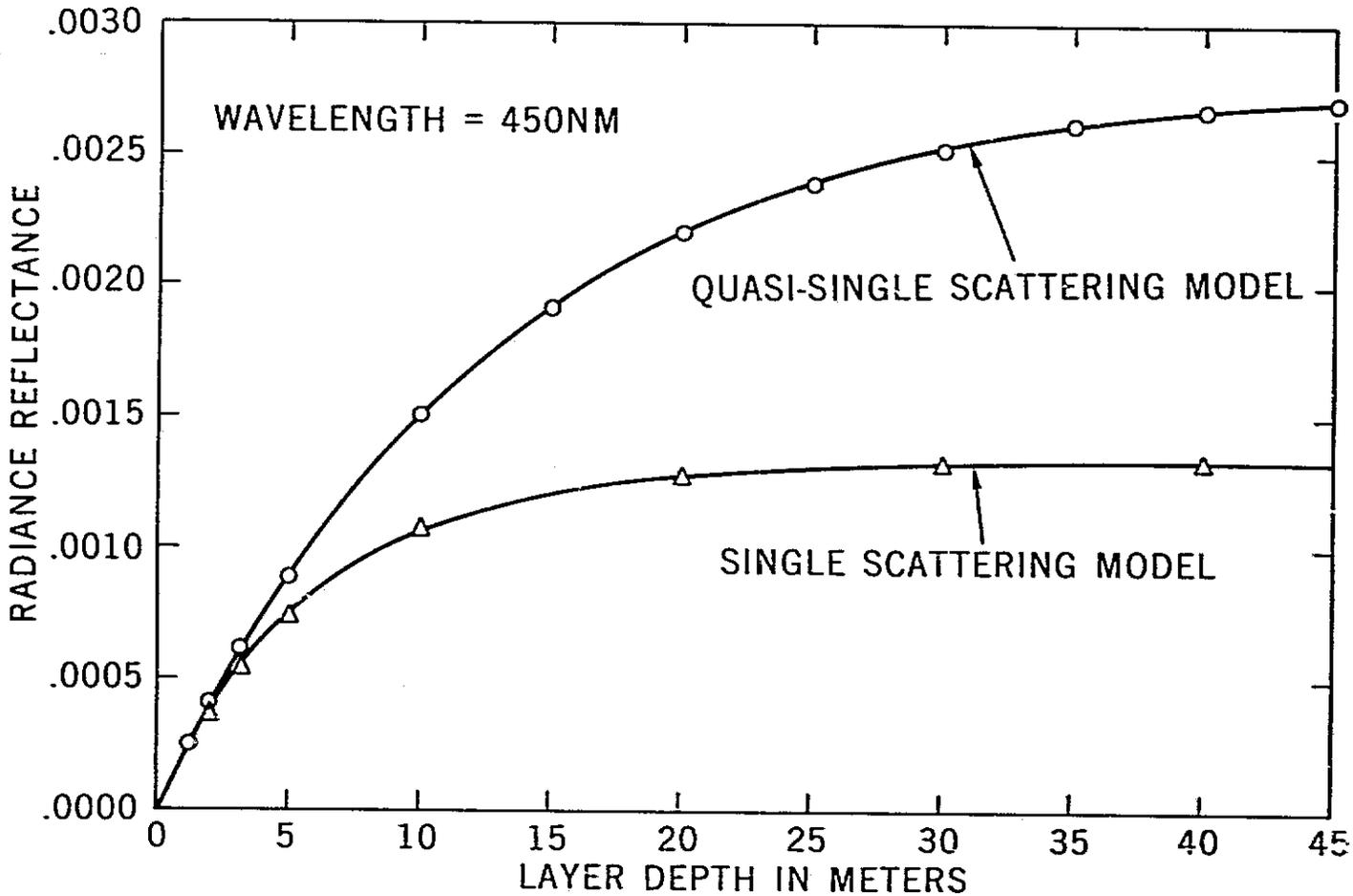

Figure 1. A Comparison of SS and QSS Models in Calculations of the Radiance Reflectance as a Function of Layer Depth for Clear Ocean Water at 450nm with a Zenith Sun.

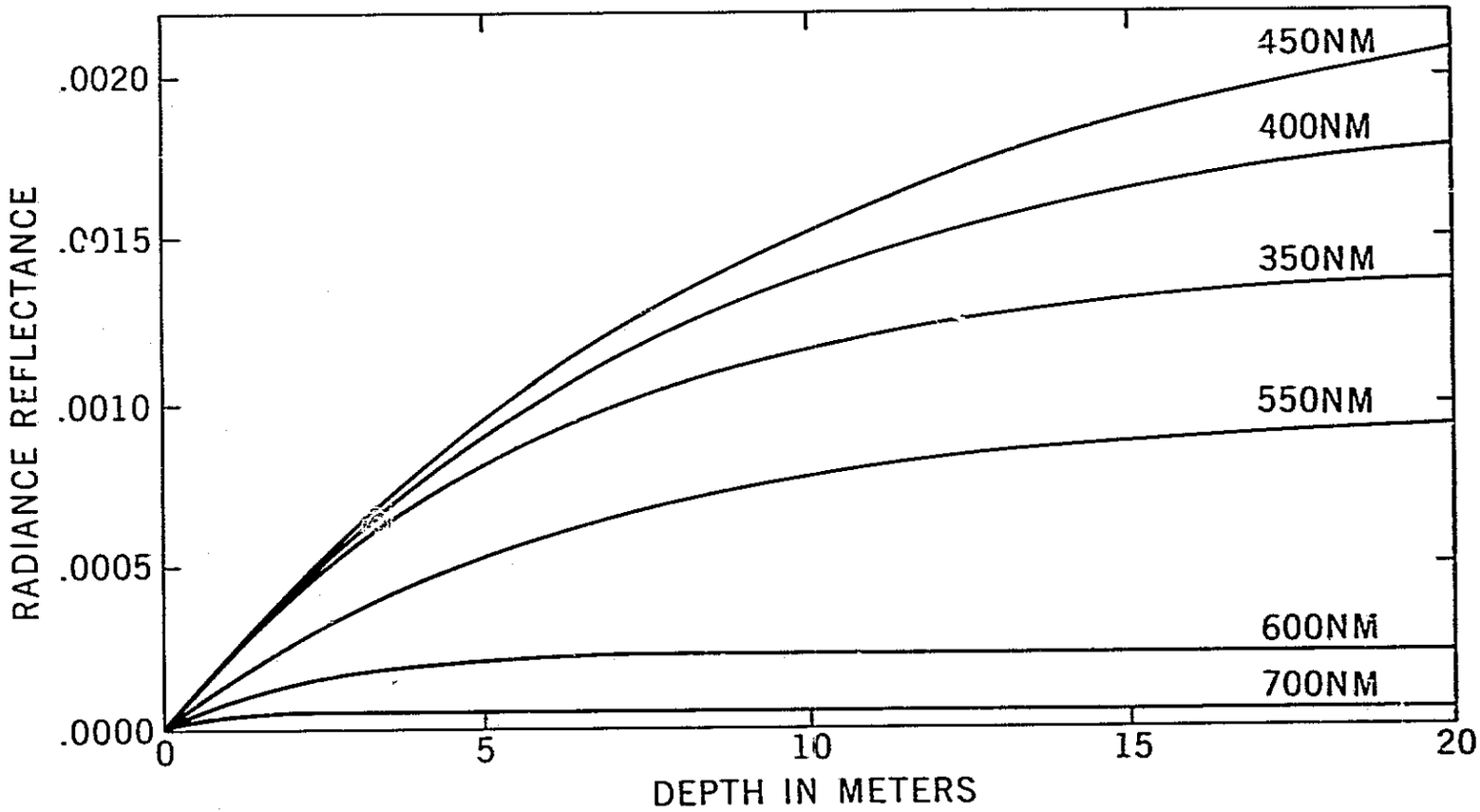

Figure 2. QSS Model Prediction of the Radiance Reflectance as a Function of Layer Depth for Clear Ocean Water at Several Wavelengths and for a Zenith Sun.

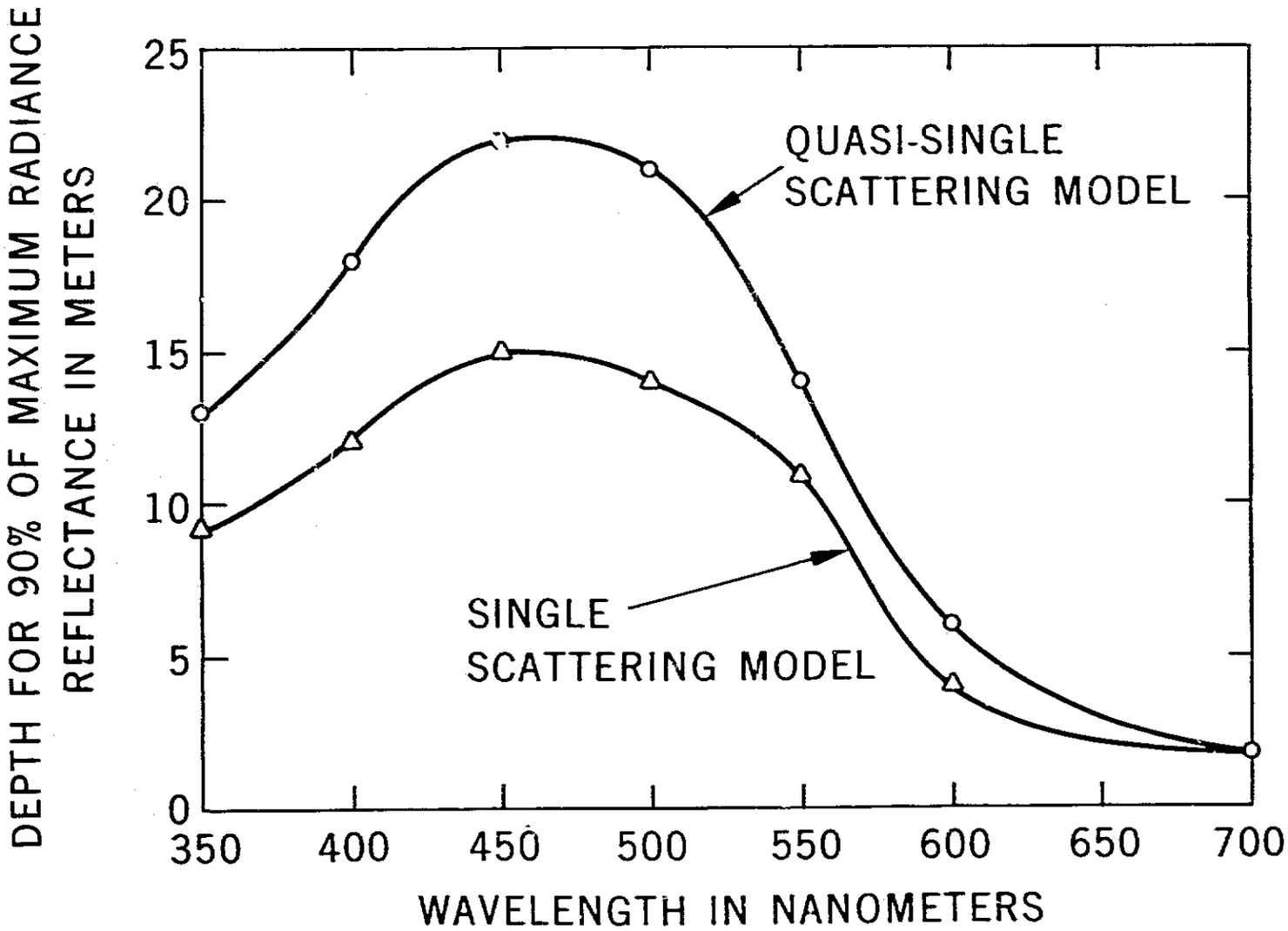

Figure 3. SS and QSS Model Penetration Depths for Clear Ocean Water as a Function of Wavelength for a Zenith Sun, Assuming no Atmosphere and a Perfectly Flat Sea Surface.

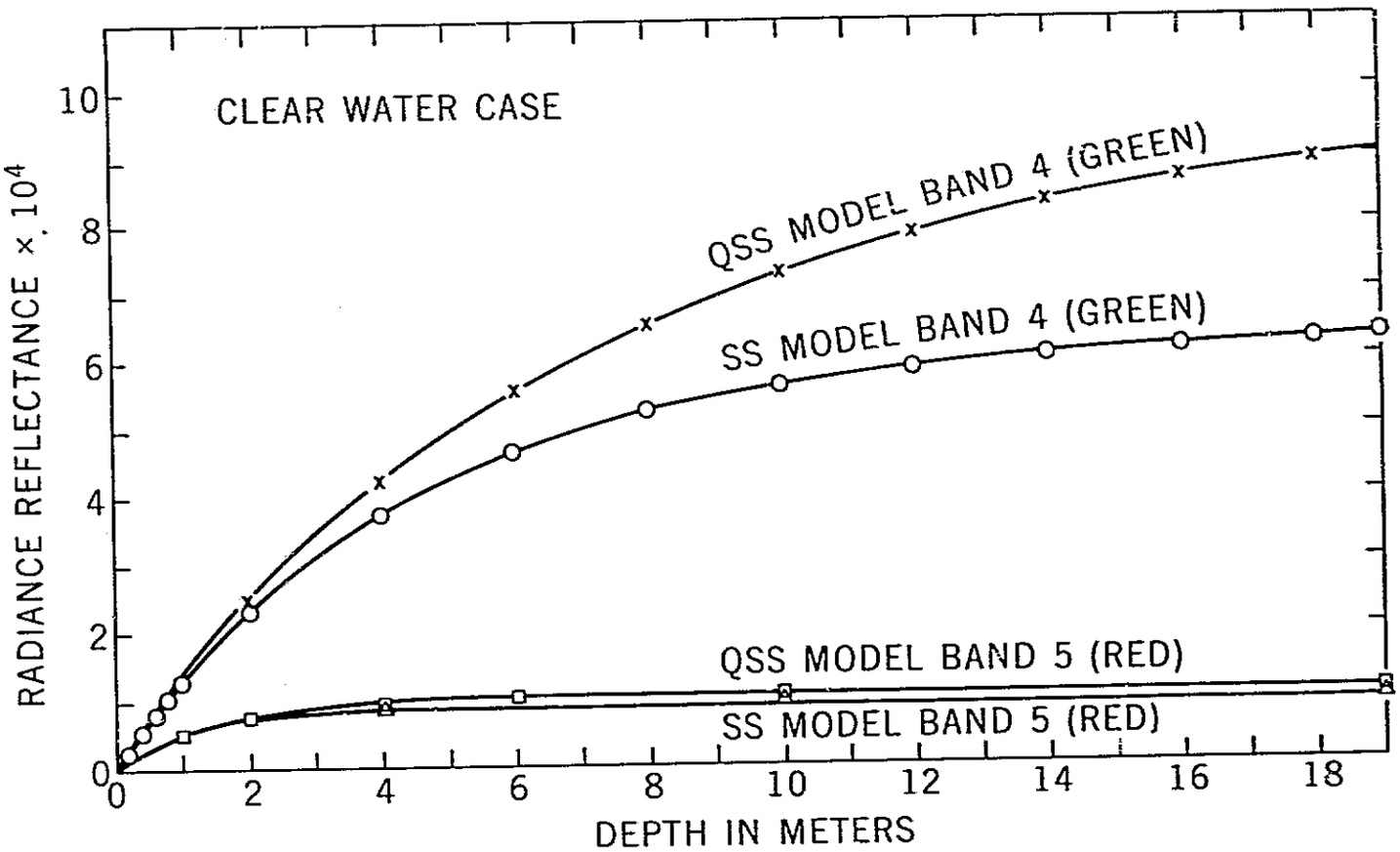

Figure 4. SS and QSS Model Radiance Reflectance Versus Layer Depth Averaged Over the Two Visible–Wavelength ERTS-1 MSS Bands for Clear Ocean Water and a Solar Zenith Angle of 30 Degrees.

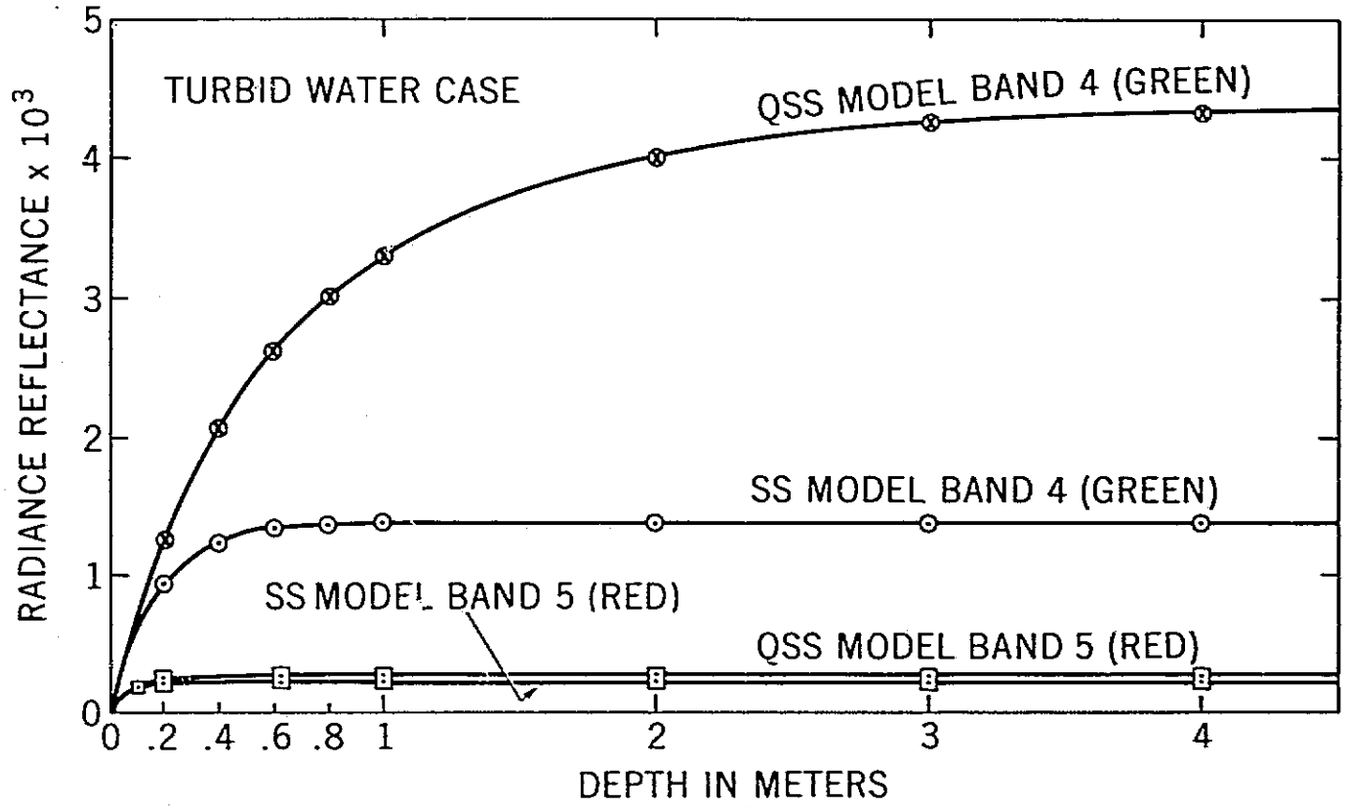

Figure 5. SS and QSS Model Radiance Reflectances Versus Layer Depth Averaged Over the Two Visible–Wavelength ERTS-1 MSS Bands for Turbid Water and a Solar Zenith Angle of 30 Degrees.

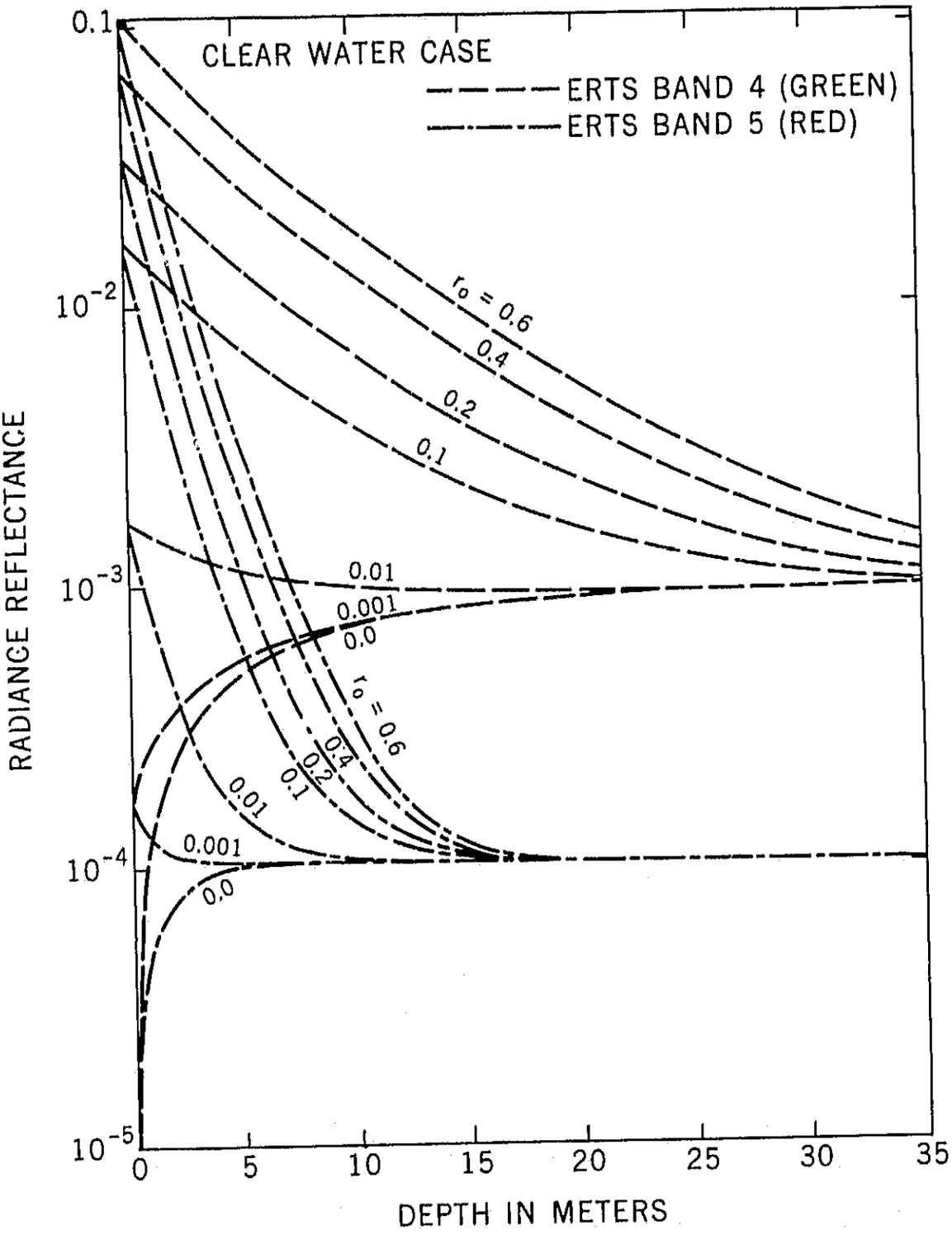

Figure 6. QSS Model Radiance Reflectances Versus Layer Depth Averaged Over the ERTS-1 MSS Bands for Clear Water and Several Different Bottom Albedos r_0.

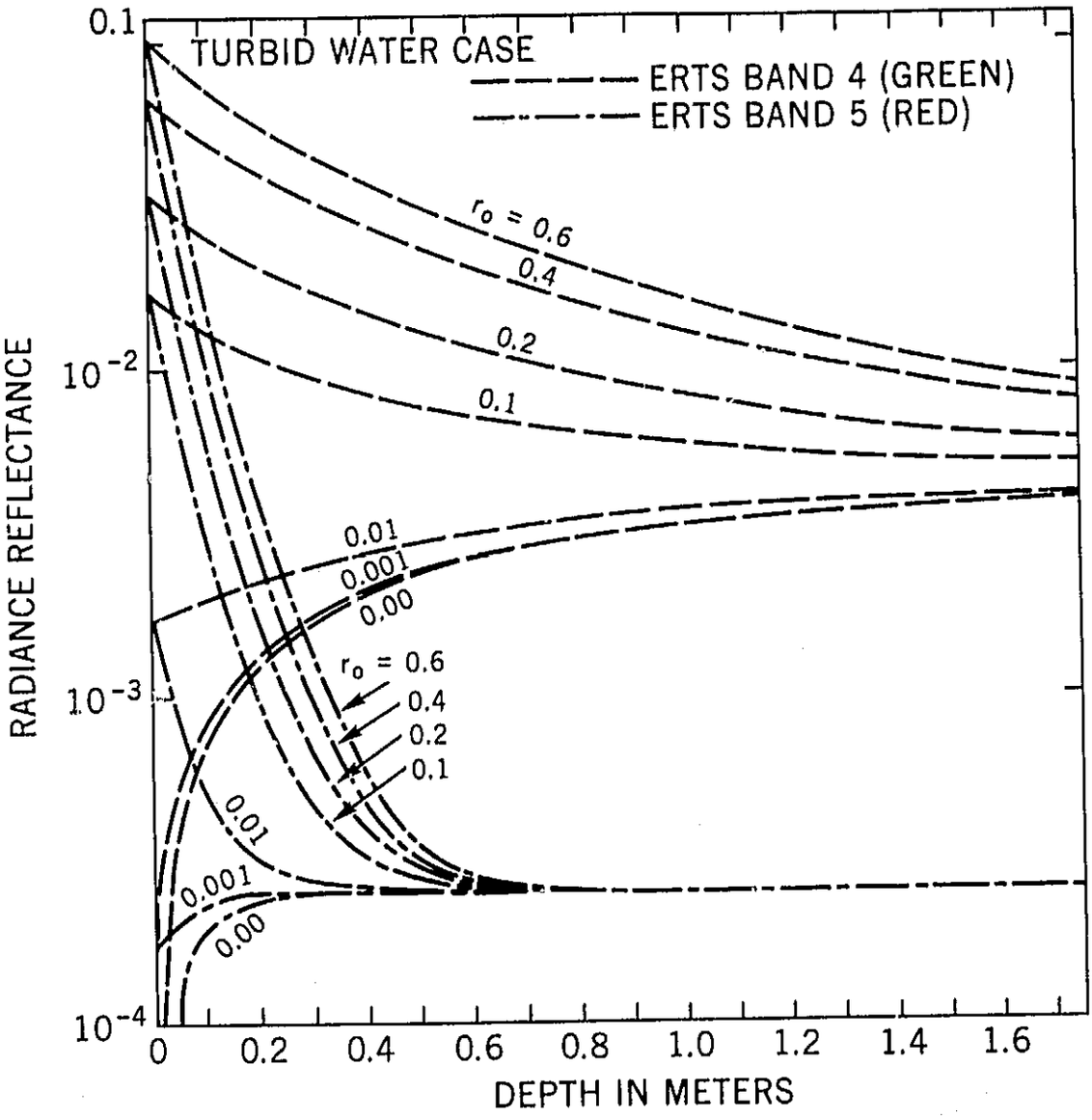

Figure 7. QSS Model Radiance Reflectances Versus Layer Depth Averaged Over the ERTS-1 MSS Bands for Turbid Water and Several Different Bottom Albedos r_0.

NASA--GSFC